産業技術研究(江原大學校 産業技術研究所 論文集) 第14輯 (1994)
Research Report, The Institute of Industrial Technology, Kangwon Nat'l Univ., Korea, Vol. 14, 1994

# The Behavior of Negative Ions in Silane Plasma Chemical Vapor Deposition

**Kyo-Seon Kim ***

# 실란 플라즈마 화학증착에서의 음이온거동

김 교 선*

## ABSTRACT

The objective of this research is to analyze the phenomena of negative ion behavior in silane plasma chemical vapor deposition. Based on the plasma chemistry, the model equations for the formation and transport of negative ions were proposed and solved. The evolutions of gaseous species along the reactor were presented for several conditions of process variables such as reactor pressure, total gas flow rate, and electric field. Based on the model results, it is found that :

(1) The concentration profiles of positive ions show the sharp peaks at the center of plasma reactor.
(2) Most of negative ions are located in bulk plasma region, because the negative ions are excluded from the sheath region by electrostatic repulsion.

## 1. Introduction

The industrial plasma processes are widely used for deposition, etching, and sputtering in device fabrication. The plasma process is notorious as one of the dirtiest processes used in microelectronics production. Particle contamination problem in various plasma processes induces several severe effects on device performance, quality and cost of final products. Dust particles formed in plasma processes can range from submicron to micron sizes and we believe there are

* 강원대학교 공과대학 화학공학과 조교수

two pathways for particle formation in plasma processes : by the plasma chemistry in the gas phase and by the fracture of deposited thin films from the tool walls and electrodes. The dust particles can be formed in the gas phase by nucleation from the chemical species inside the plasma reactor. The dust particles can also be formed from the fracture of thin films by thermal and electrical stresses induced by the plasma. Those particles in a plasma will gain negative charges by collision of hot electrons, be trapped inside the plasma by electrostatic repulsion from the sheath region, and will grow to larger particles[1-26].

Recently, it is believed that the polymerized negative ions are the precursor of dust particles. In this research, we concentrated on the pathway of particle formation by the plasma chemistry in the gas phase and analyzed the negative ion formation, growth and transport in plasma reactor. We included the plasma chemistry of silane and transport of chemical species.

There are 3 general approaches for plasma modeling : (1) fluid approach based on the general tranport equations, (2) kinetic approach based on particle-in-cell/Monte Carlo simulation and (3) hybrid Monte Carlo/fluid model[13-21, 27-30]. The second and third methods are, more or less, related with Monte Carlo simulation and are expensive compuationally and we decided to work on fluid approach for plasma modeling. Also it is assumed that the electron number concentration and electron energy are uniform inside the reactor and the electric field is given as a function of position only and we neglected the time variant effects of electric field inside the plasma reactor.

Based on literature survey, there are no other published results about particle contamination problems in plasma system, considering all those relevant topics together such as plasma reaction chemistry for cluster formation, particle formation, particle growth and transport in plasma reactor. Recently, some published papers are found to discuss about just one or two of those relevant topics. In this analysis, all those important phenomena were included for negative ion evolutions from plasma reaction chemistry to negative ion transport.

## 2. Chemical Reactions for Negative Ions in PCVD of Silane

To describe the plasma chemistry and reactions in PCVD of silane completely, more than 50 chemical species and more than 200 chemical reactions will be needed[9-12, 15, 31-38]. As the main purpose of this research is focused on the predicton of negative ion formation and transport, we tried to discard all those chemical reactions which are less important for negative ion formation and growth.

To select the important chemical reactions for particle formation from plasma chemistry of $SiH_4$, it is assumed that the negative ions have more pivotal role for the particle formation and growth than the neutrals and positive ions in plasma[10-12, 16]. It is also suggested experimentally that polymerization pathway in PCVD of $SiH_4$ will proceed via negative

ion clustering, based on several experimental observations : no neutrals as high as negative ions in mass were detected, the very different abundance ratio between negative ions and neutrals cannot be explained by imposing attachment reaction and no attachment reaction were measured for negative ions heavier than trisilicon hydride anions[10-12].

By discarding some chemical reactions which are not important for particle formation, we could end up with 18 chemical species and 23 chemical reactions. The following 23 chemical reactions are considered in our modeling to predict the particle formation and growth in PCVD of $SiH_4$[9-12, 15, 31-38].

$SiH_4 + e \xrightarrow{4\times10^{-13}} SiH_x^- (SiH_2^- \text{ or } SiH_3^-) + (H \text{ or } H_2)$ (R1)

$SiH_4 + e \xrightarrow{2\times10^{-10}} SiH_x \text{ (neutrals)} + (H \text{ or } H_2)$ (R2)

$SiH_4 + e \xrightarrow{1.43\times10^{-11}} SiH_x^+ + (H \text{ or } H_2)$ (R3)

$SiH_4 + e \xrightarrow{8.34\times10^{-9}} SiH_4 (v2, 4) + e$ (R4)

$SiH_4 + e \xrightarrow{8.74\times10^{-9}} SiH_4 (v1, 3) + e$ (R5)

$SiH_4 (v2, 4) + H_2 \xrightarrow{3.05\times10^{-12}} SiH_4 + H_2$ (R6)

$SiH_4 (v1, 3) + H_2 \xrightarrow{6.08\times10^{-11}} SiH_4 (v2, 4) + H_2$ (R7)

$SiH_x^+ + e \xrightarrow{1.68\times10^{-7}} SiH_x \text{ (neutrals)} + H$ (R8)

$SiH_x + e \xrightarrow{4\times10^{-13}} SiH_x^-$ (R9)

$SiH_x^- + SiH_x^+ \xrightarrow{5\times10^{-7}} Si_2H_{x'}^- \text{ (neutrals)} + (H \text{ or } H_2)$ (R10)

$Si_nH_x^- \xrightarrow{+SiH_4,\, k_n} Si_{n+1}H_{x'}^- + (H \text{ or } H_2)$ (n : 1~13) (R11-23)

($k_1=10^4$, $k_2=2.5\times10^3$, $k_3=2.8\times10^3$, $k_4=3.2\times10^3$, $k_5=3.6\times10^3$, $k_{6\text{-}13}=4\times10^3$)

## 3. Governing Equations for Gas Species in Silane PCVD

For our numerical calculation, we used the experimental reactor proposed by Watanabe[39]. The plasma reactor by Watanabe[39] is designed to observe the particle formation, growth and trans-port in PCVD of $SiH_4$. He used the powered electrodes and ground electrodes made of stainless steel and both electrodes have perforations so that the input and output gas can pass through the electrodes. The gas stream is flowing upward (opposite to the direction of gravity). The powered electrode is located upstream of the grounded electrode. We can expect the plug flow (1-dimensional flow) inside the reactor by these perforated electrodes. As we are dealing with many chemical reactions already, it is absolutely required to simplify the fluid model equations as much as possible. By using the ideal reactor proposed by Watanabe[39] as our model reactor, we could neglect the momentum balance equation from our model equations. By assuming a 1-D flow in our model equations, we could reduce the required computational time abruptly.

The governing equations for gaseous chemicals, i, such as neutrals, radicals and ionic species are expressed as Eq. 1, considering chemical reactions, convection, electric migration and diffusion.

$$\frac{\partial N_i}{\partial t} = (RXN)_i - \nabla \cdot (uN_i - \delta_i \mu_i E N_i - D_i \nabla N_i) \quad (1)$$

The first term on RHS terms in Eq. 1 is the generation rate of chemical species by the chemical reactions. The second term shows the effect of fluid convection and the third term is the effect of electrical migration of ionic species under the electric field of plasma. The electrical migration coefficients ($\mu_i$) of ionic species was calculated by the Einstein relationship as[40] :

$$\mu_i = \frac{z_i D_i}{k_B T} \cdot \quad (2)$$

The $\delta_i$ is given as 1 for positive ion, -1 for negative ion and 0 for neutral species and $z_i$ is the number of charges for ionic species. The time-averaged electric field (E) inside rf plasma reactor was expressed as a function of axial distance as follows, by adopting the computed results for average electric field from literature[30] and also by applying the Child-Langmuir equation for collisionless plasma sheath[41] :

$$E = E_{pos}\left[1 - \left(\frac{x}{x_{pos}}\right)^{1/3}\right] \text{ for } 0 \le x < x_{pos} \quad (3)$$

$$E = 0 \quad \text{for } x_{pos} \le x < x_{neg} \quad (4)$$

$$E = E_{neg}\left[1 - \left(\frac{x_{end} - x}{x_{end} - x_{neg}}\right)^{1/3}\right] \quad \text{for } x_{neg} \le x \le x_{end} \cdot \quad (5)$$

The last term on RHS in Eq. 1 shows the effect of gas species diffusion in axial direction and the diffusion coefficients of chemical species were calculated by the Chapman and Enskog equation as[42] :

$$D_i = 1.858 \times 10^{-3} T^{3/2} \left[\frac{(1/M_A + 1/M_B)}{p\sigma_{AB}^2 \Omega_D}\right]^{1/2} \quad (6)$$

$$\sigma_{AB} = (\sigma_A + \sigma_B)/2 \quad (7)$$

$$\Omega_D = \frac{A}{T^{*B}} + \frac{C}{\exp(DT^*)} + \frac{E}{\exp(FT^*)} + \frac{G}{\exp(HT^*)} \quad (8)$$

$$T^* = \frac{k_B T}{\varepsilon_{AB}} \quad (9)$$

$$\varepsilon_{AB} = (\varepsilon_A \varepsilon_B)^{1/2} \quad (10)$$

where A=1.06036, B=0.15610,
C=0.19300, D=0.47635,
E=1.03587, F=1.52996,
G=1.76474, H=3.89411.

The Lennard-Johnes potential parameters for $SiH_4$ were available in the literature[42] and, for the remaining silicon containing species, were estimated by scaling to analogous carbon-containing species.

We assumed that the plasma reactor is supplied with pure $SiH_4$ and the concentrations of all the other chemical species were assumed to be zero as initial conditions. As boundary conditions at electrode walls, we assumed that the sticking coefficients of positive ions are unity and the sticking coefficients of positive and neutrals are zero[13-20, 27-28, 30].

By appling the finite difference at P mesh points for spatial variable (x) only, the 18 partial differential equations for chemical species are converted into 18xP ordinary differential equations (ODEs). The 18xP ODEs are solved by the effi-

cient ODE solver, GEAR subroutine.

## 4. Results and Discussion

The numerical simulation of the model equations proposed in previous section was performed for the following process conditions and reactor parameters :

total gas flow rate=50㎖/sec.,
pressure=0.2torr,
$E_{pos}$ = 3 volt/㎝, $E_{neg}$ = -3 volt/㎝,
reactor length ($x_{end}$) = 2㎝,
reactor temperature (T) = 800K,
reactor diameter = 8.5㎝.

All those process conditions except for $E_{pos}$ and $E_{neg}$ are in the range of typical reactor conditions for amorphous Si deposition by PCVD. The model equations for ionic species are so sensitive to the changes of $E_{pos}$ and $E_{neg}$, and we need to increase the number of meshes at high value of $E_{pos}$ and $E_{neg}$ for the stable solution of mode equations. For these standard conditions of $E_{pos}$ =3 volt/㎝ and $E_{neg}$ =-3 volt/㎝, we needed, at least, 23 meshes and the computational time required at HP workstation was about 2 hrs to reach the steady states at t ≅ 0.02sec. The $E_{pos}$ and $E_{neg}$ in industrial PCVD reactor would be around +100 volt/㎝ and -100 volt/㎝, respectively, and the number of meshes required for the stable solution is more than 200 and the computational time would increase by 450 times, comparing to the computational time in standard conditions. Because of the high cost of computational time for high values of $E_{pos}$ and $E_{neg}$ we decided to analyze the effects of electric field, qualitatively, by changing the $E_{pos}$ and $E_{neg}$ at low values.

Fig. 1 shows the evolution of $SiH_4$ concentration along the reactor length for various times. It is assumed that the reactor is filled with pure $SiH_4$ initially and, as time (t) increases, the $SiH_4$ concentration decreases by chemical reactions and reaches the steady state concentration about=0.02 sec. The pure

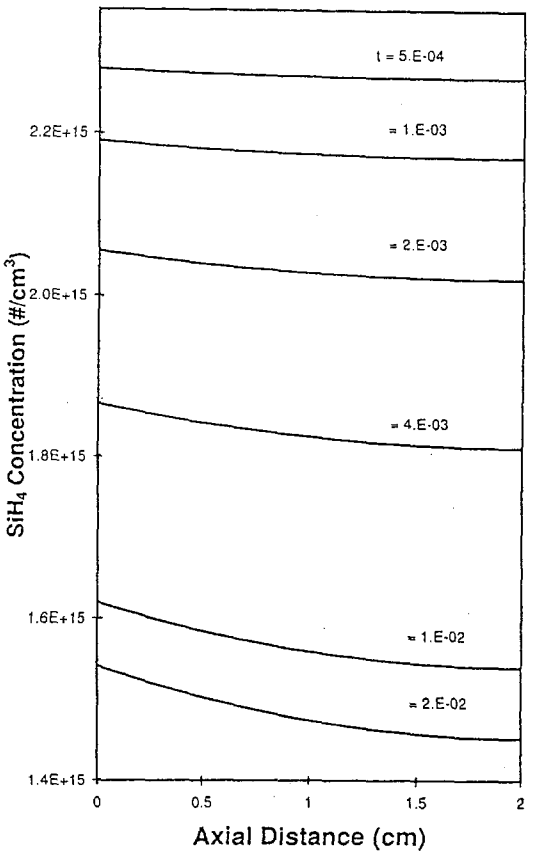


**Fig. 1. The evolution of SiH concentration profiles along the axial distance for various times.**

$SiH_4$ is supplied at the reactor inlet (x=0) and the $SiH_4$ concentration decreases by chemical reaction as the axial distance of reactor increases. The change of $SiH_x$ neutral concentration inside the reactor is shown in Fig. 2. The concentration of $SiH_x$ at the center of reactor is higher than in the region near electrode wall, because the $SiH_x$ is formed inside the reactor and lost by diffusion towards the electrodes. The $SiH_x^+$ concentration increases very quickly by fast ionization reaction before t=5.E-04 sec. and decreases, after then, by the ion-ion reaction, electrical migration and diffusion to reach the steady state at t=0.02 sec. (Fig. 3). The $SiH_x^+$ concentration at the center of reactor shows a steeper peak than the $SiH_x$ concentration, because the $SiH_x^+$ is lost towards the electrodes by fast electrical migration and diffusion rates.

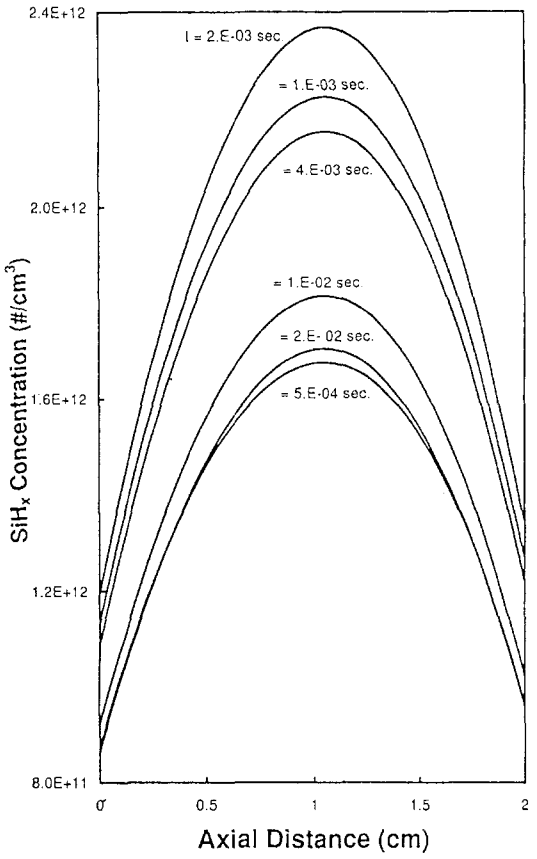


**Fig. 2. The evolution of $SiH_x$ concentration profiles along the axial distance for various times.**

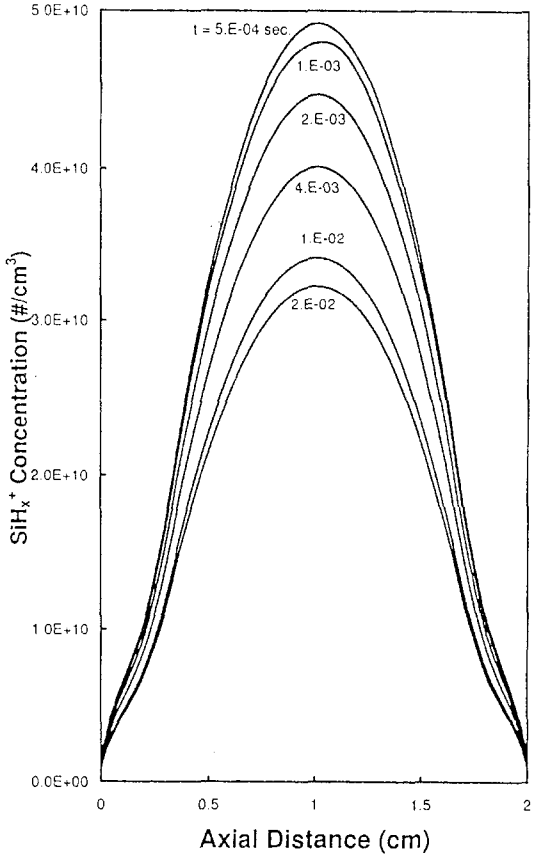


**Fig. 3. The evolution of $SiH_x^+$ concentration profiles along the axial distance for various times.**

The $SiH_x^-$ concentration shows two peaks on both sides of sheath boundaries, because the $SiH_x^-$ formed in sheath regions is excluded from sheath regons by the electrostatic repulsion and accumulated at the sheath boundaries (Fig. 4). The $SiH_x^-$ concentration at the center of reactor is balanced by chemical generation and disapperance rates, and transport rates by diffusion and convection. The $SiH_x^-$ concentration at the center of reactor is shown to be lower than at the sheath boundaries.

Figs. 5-8 show the evolutions of $Si_2H_x^-$, $Si_7H_x^-$, $Si_{10}H_x^-$, and $Si_{13}H_x^-$ concentrations, respectively, along the reactor distance and those concentrations are higher in the bulk plasma region than at the sheath region, because the negative ions are extracted from the sheath region by the electrostatic repulsive force. As the number of silicon atom increases in

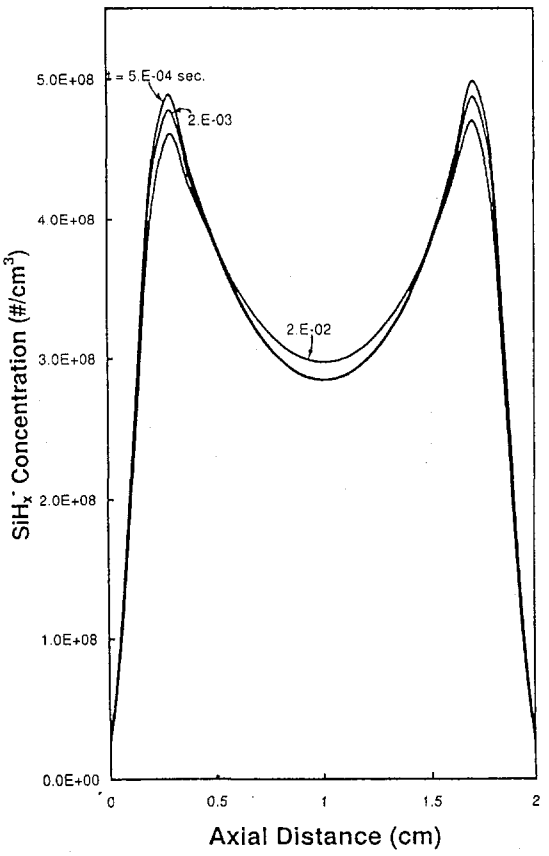


**Fig. 4. The evolution of $SiH_x^-$ concentration profiles along the axial distance for various times.**

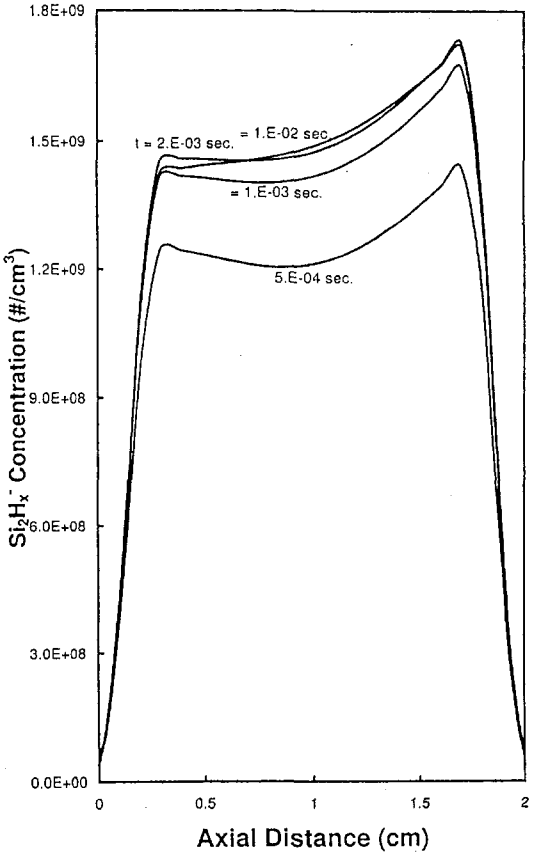


**Fig. 5. The evolution of $Si_2H_x^-$ concentration profiles along the axial distance for various times.**

chain reactions, it takes more time for the polymerization reaction to take place, propagating through the chain reactions (R 11-23), and the concentrations of higher mass negative ions increase more slowly than those of lower mass negative ions. For example, the $Si_7H_x^-$ starts to increase in concentration at t=5.E-04 sec., $Si_{10}H_x^-$ at t=1.E-03 sec., and $Si_{13}H_x^-$ at t=1.5E-03 sec. and they reach the steady state concentrations at t=1.E-02 sec. The concentrations of $Si_nH_x^-$ at the sheath boundary of downstream (x=1.7 *cm*) are higher than those of upstream (x =0.3*cm*), because the fluid carries those chemical species towards the downstream.

## 5. Conclusions

The model equations to predict negative ion formation and transport in rf PCVD

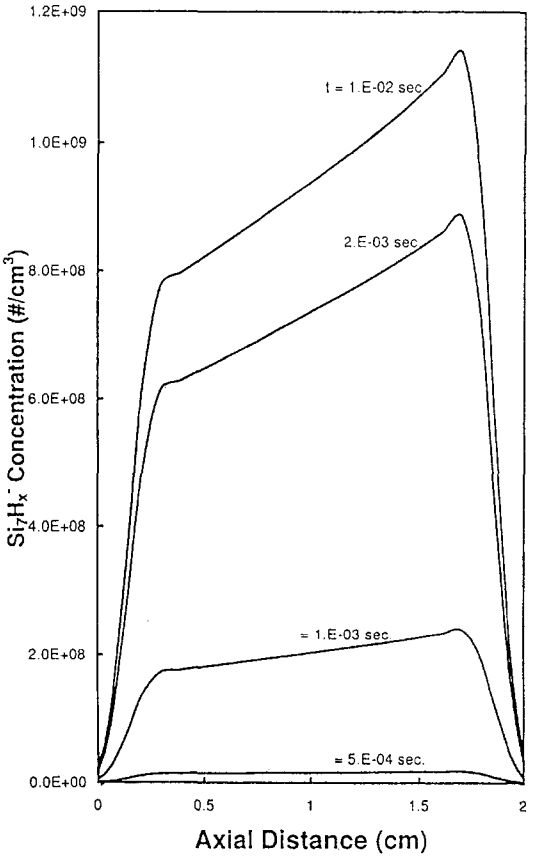


**Fig. 6. The evolution of $Si_7H_x^-$ concentration profiles along the axial distance for various times.**

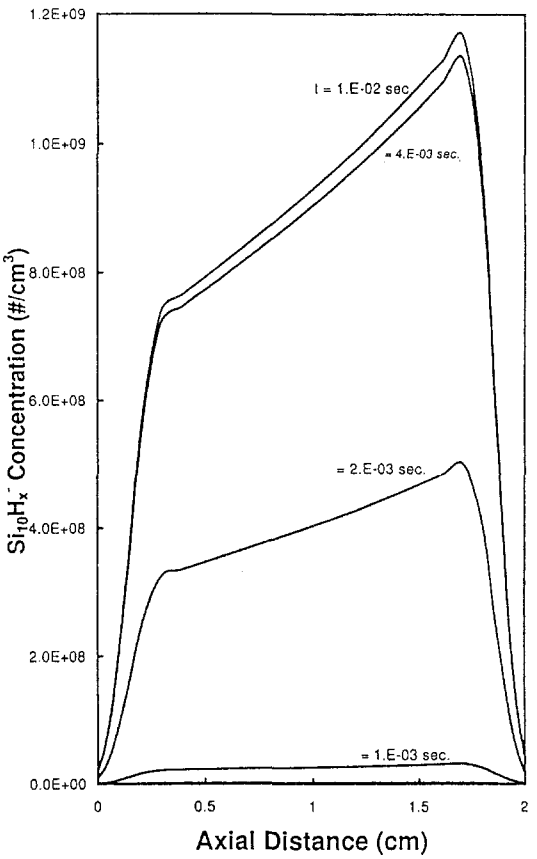


**Fig. 7. The evolution of $Si_{10}H_x^-$ concentration profiles along the axial distance for various times.**

reactor with $SiH_4$ were proposed in this study. The major physical phenomena considered in model equations are : plasma chemical reactions related with cluster formation, convection, diffusion and electrical migration of gas species. The evolutions of gaseous species along the reactor were presented and the important results in this research are :

o It takes 0.02 second for all chemical species to reach the steady state at standard process conditions in these simulations.

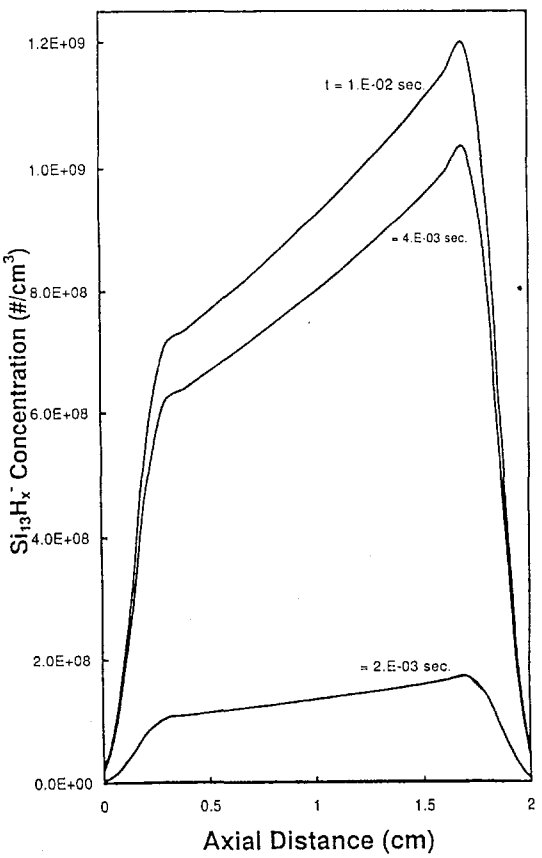


**Fig. 8. The evolution of $Si_{13}H_x^-$ concentration profiles along the axial distance for various times.**

o The positive ions are formed inside the reactor and lost very fast to both electrodes and the profiles of positive ions show sharp peaks at the center of reactor.

o The negative ions are excluded from the sheath region by electrostatic force and are accumulated in bulk plasma region. The concentration profiles of negative ions are very steep in sheath region but are flattened in the bulk region.

o The negative ions of higher mass are generated later than those of lower mass, because it takes more time for the polymerization reaction of higher mass negative ions to occur through the chain reaction.

As it takes long computational time to get the results with the actual values of $E_{pos}$ and $E_{neg}$ (about $\pm 100$ volt/$cm$), we assumed the lower values of $E_{pos}$ and $E_{neg}$ ($\leq \pm 4$ volt/$cm$). It is absolutely required to find a numerical scheme to reduce the computational time with the actual values of $E_{pos}$ and $E_{neg}$. We need to find more elaborate numerical scheme to improve numerical computational efficiency for this complicated problem, where the transport phenomena and chemical reactions are coupled.

We just selected the plasma chemical reactions that might be important for the particle formation, growth and transport in silane PCVD. To have better predictive results in plasma chemistry, more chemical reactions should be included in model equations, but, in this case, it will

cost more computational time. We also assumed that the electron concentration and kinetic energy are uniform inside the reactor, but they will change as a function of time and position. In that sense, our model equations are not self-consistent. We can improve the accuracy of model results by adding the model equations for electron concentration and energy, but it will also add lots of computational time and we will, again, need to find more efficient numerical scheme.

## Nomenclature

| | |
|---|---|
| D | diffusitivity, $cm^2$/sec. |
| E | electric field in plasma reactor, volt/$cm$. |
| $E_{pos}$ | maximum avearge electric field in rf plasma at powered electrode, volt/$cm$. |
| $E_{neg}$ | minimum avearge electric field in rf plasma at ground electrode, volt/$cm$. |
| $k_B$ | Boltzmann constant. |
| $k_n$ | chemical reaction constant for the n-th chemical reaction. |
| $M_A$ , $M_B$ | molecular weight of chemical species, A and B. |
| N | number concentration of chemical species, #/$cm^3$. |
| p | pressure, atm. |
| P | number of mesh points for computation. |
| RXN | chemical reaction rate, / $cm^3$ sec. |
| t | time, sec. |
| T | temperature, K. |
| u | gas stream velocity, $cm$/ sec. |
| x | axial distance of reactor, $cm$. |
| $x_{end}$ | reactor length in axial direction, $cm$. |
| $x_{pos}$ | axial distance where the average plasma electric field becomes zero near powered electrode, $cm$. |
| $x_{neg}$ | axial distance where the average plasma electric field becomes zero near ground electrode, $cm$. |
| z | number of charges of chemical species. |

## Greek Letters

| | |
|---|---|
| $\delta$ | identification of ionic species ($\delta = 1$ for positive ion, $\delta = 0$ for neutrals, $\delta = -1$ for negative ion). |
| $\varepsilon_A, \varepsilon_B$ | Lennard-Jones well depth. |
| $\mu$ | electrical mobility. |
| $\sigma_A, \sigma_B$ | Lennard-Jones characteristic length. |
| $\Omega_D$ | diffusion collision integral. |

## Subscripts

| | |
|---|---|
| i | i chemical species. |

## References


1. Watanabe, Y., M. Shiratani, Y. Kubo, I. Ogawa and S. Ogi, "Effects of low-frequency modulation on rf discharge chemical vapor deposition", *Appl. Phys. Lett.*, *53* (14), 1263 (1988).

2. Shiratani, M., S. Matsuo and Y. Watanabe, "In Situ Observation of Particle Behavior in rf silane plasmas", *Jpn. J. Appl. Phys.*, *30* (8), 1887 (1991).
3 Shiratani, M., T. Fukuzawa, K. Eto and Y. Watanabe, "Detection of negative ions in a helium-silane RF plasma", *Jpn. J. Appl. Phys. Part2*, *31* (12B), L1791 (1992).
4. Watanabe, Y. and M. Shiratani, "Growth kinetics and behavior of dust particles in silane plasmas", *Jpn. J. Appl. Phys. Part 1*, *32* (6B), 3074 (1993).
5. Selwyn, G. S., J. Singh and R. S. Bennett, "In situ laser diagonostic studies of plasma-generated particulate contamination", *J. Vac. Sci. Technol A7* (4), 2758 (1989).
6. Selwyn, G. S., J. S. McKilop, K. L. Haller and J. J. Wu, "In situ plasma contamination measurements by HeNe laser scattering : a case study", *J. Vac. Sci. Technol A8* (3), 1726 (1990).
7. Selwyn, G. S., "Plasma particulate contamination control. I. Transport and process effects", *J. Vac. Sci. Technol.*, *B9* (6), 3487 (1991).
8. Selwyn, G. S., and E. F. Patterson, "Plasma particulate contamination control. II. Self-cleaning tool design", *J. Vac. Sci. Technol.*, *A10* (4), 1053 (1992).
9. Dorier, J-L., Ch. Hollenstein, A. A. Howling and U. Kroll, "Powder dynamics in very high frequency silane plasmas", *J. Vac. Sci. Technol.*, *A10* (4), 1048 (1992).
10. Howling, A. A., J. -L. Dorier, and Ch. Hollenstein, "Negative ion mass spectra and particulate formation in radio frequency silane plasma deposition experiments", *Appl. Phys. Lett.*, *62* (12), 1341 (1993).
11. Howling, A. A., L. Sansonnens, J. -L. Dorier, and Ch. Hollenstein, "Negative hydrogenated silicon ion clusters as particle precursors in RF silane plasma deposition experiments", *J. Phys. D : Appl. Phys.*, *26*, 1003 (1993).
12. Howling, A. A., L. Sansonnens, J. -L. Dorier and Ch. Hollenstein, "Time-resolved measurements of highly polymerized negative ions in radio frequency silane plasma deposition experiments", *J. Appl. Phys.*, *75* (3), 1340 (1994).
13. Choi, S. J., M. J. McCaughey, and T. J. Sommerer, "Perturbation of the cathode fall in direct-current glow discharges by particulate contamination", *Appl. Phys. Lett.*, *59* (24), 3102 (1991).
14. Sommerer, T. J., M. S. Barnes, J. H. Keller, M. J. McCaughey, and M. J. Kushner, "Monte Carlo-fluid hybrid model of the accumulation of dust particles at sheath edges in radio-frequency discharges", *Appl. Phys. Lett.*, *59* (6), 638 (1991).
15. Kusher, M. J., "A model for the discharge kinetics and plasma chemistry during plasma enhanced chemical vapor deposition of amorphous silicon", *J. Appl. Phys.*, *63* (8), 2532 (1988).
16. Choi, S. J., and M. J. Kushner, "The

role of negative ions in the formation of particles in low-pressure plasmas", *J. Appl. Phys.*, *74* (2), 853 (1993).

17. Choi, S. J., and M. J. Kushner, "Simulation of the shielding of dust particles in low pressure discharges", *Appl. Phys. Lett.*, *62* (18), 2197 (1993).
18. Jellum, G. M., J. E. Daugherty, and D. B. Graves, "Particle thermophoresis in low pressure glow discharges", *J. Appl. Phys.*, *69* (10), 6923 (1991).
19. Daugherty, J. E., R. K. Porteous, M. D. Kilgore, and D. B. Graves, "Sheath structure around particles in low-pressure discharges", *J. Appl. Phys.*, *72* (9), 3934 (1992).
20. Kilgore, M. D., J. E. Daugherty, R. K. Porteous, and D. B. Graves, "Ion drag on an isolated particulate in a low-pressure discharge", *J. Appl. Phys.*, *73* (11), 7195 (1993).
21. Barnes, M. S., J. H. Keller, J. C. Forster, J. A. O'Neill, and D. K. Coultas, "Transport of Dust particles in Glow-Discharge Plasmas", *Phys. Rev. Lett.*, *68* (3), 313 (1992).
22. Yoo, W. J. and Ch. Steinbruchel, "Kinetics of particle formation in the sputtering and reactive ion etching of silicon", *J. Vac. Sci. Technol.*, *A10* (4), 1041 (1992).
23. Yoo, W. J. and Ch. Steinbruchel, "Growth of plasma-generated particles and behavior of particle clouds during sputtering of silicon and silicon dioxide", *J. Vac. Sci. Technol.*, *A11* (4), 1258 (1993).
24. Smaldi, M. M., G. Y. Kong, R. N. Carlile and S. E. Beck, "Particle contamination on a silicon substrate in a $SF_6$/Ar plasma", *J. Vac. Sci. Technol.*, *B10* (1), 30 (1992).
25. Banerjee, R., S. N. Sharma, S. Chatto-padhyay, A. K. Batabyal and A. K. Barua, "Control of powder formation in silane discharge by cathode heating and hydrogen dilution for high-rate deposition of hydrogenated amorphous silicon thin films", *J. Appl. Phys.*, *74* (7), 4540 (1993).
26. Costa, J., P. Roura, G. Sardin, J. R. Morante and E. Bertran, "Unusual photoluminescence properties in amorphous silicon nanopowder produced by plasma enhanced chemical vapor deposition", *Appl. Phys. Lett.*, *64* (4), 463 (1994).
27. Makabe, T., N. Nakano and Y. Yamaguchi, "Modeling and diagonostics of the structure of rf glow discharges in Ar at 13.56 MHz", *Phys. Rev.*, *45*, 2520 (1992).
28. Yamaguchi, Y., A. Sumiyama, R. Hatt-ori, Y. Morokuma and T. Makabe, "A model of amorphous silicon deposition in DC glow discharge in silane", *J. Phys. D. : Appl. Phys.*, *22*, 505 (1989).
29. Tochikubo, F., A. Suzuki, S. Kakuta, Y. Terazono and T. Makabe, "Study of the structure in rf glow discharges in $SiH_4/H_2$ by spatiotemporal optical emission spectroscopy : influence of negative ions", *J. Appl. Phys.*, *68* (11), 5532 (1990).

30. Sato, N., and H. Tagashira, "A hybrid Monte Carlo/Fluid model of RF plasmas in a $SiH_4/H_2$ mixture", *IEEE Trans. Plasma Sci.*, *19* (2), 102 (1991).
31. Haller, I., "Importance of chain reactions in the plasma deposition of hydrogenated amorphous silicon", *J. Vac. Sci. Technol.*, *A1* (3), 1376 (1983).
32. Weakliem, H. A., R. D. Estes and P. A. Longeway, "Ion-molecule reactions in a direct current silane glow discharge", *J. Vac. Sci. Technol.*, *A5* (1), 29 (1987).
33. Vanier, P. E., F. J. Kampas, R. R. Cord-erman and G. Rajeswaran, "A study of hydrogenated amorphous silicon deposited by rf glow discharge in silane-hydrogen mixtures", *J. Appl. Phys.*, *56* (6), 1812 (1984).
34. Doughty, D. A. and A. Gallagher, "Ca-uses of $SiH_4$ dissociation in silane dc discharges", *Phys. Rev. A*, *42*, 6166 (1990).
35. Doughty, D. A. and A. Gallagher, "Sp-atial distributions of a-Si : H film-producing radicals in silane rf glow discharges", *J. Appl. Phys.*, *67* (1), 139 (1989).
36. Gallagerer, A., "Neutral radical deposition from silane discharges", *J. Appl. Phys.*, *63* (7), 2406 (1988).
37. Matsuda, A. and K. Tanaka, "Investigation of the growth kinitics of glow-discharge hydrogenated amorphous silicon using a radical separation technique", *J. Appl. Phys.*, *60* (7), 2351 (1986).
38. Scott, B. A., J. A. Reimer and P. A. Longeway, "Growth and defect chemistry of amorphous hydrogenate silicon", *J. Appl. Phys.*, *54* (12), 6853 (1983).
39. Watanabe, Y, *personal communication* (1994).
40. Chen, F. F., *Introduction to plasma Physics and Controlled Fusion*, 2nd ed., Plenum press, New York (1984).
41. Chapman, B., *Glow Discharge Processes : Sputtering and Plasma Etching*, John Wiley & Sons, New York (1980).
42. Reid, R. C., J. H. Prausnitz, and T. K. Sherwood, *The Properties of Gases and Liquids*, 3rd ed., McGraw-Hill, New York (1977).